Experiments Designed to Assess the Margin-to-Failure of Steel Containments Susceptible to "Knuckle" Buckling

G. Fly, J.G. Bennet, W.E. Baker
Los Alamos National Laboratory, MS/J576, P.O. Box 1663, Los Alamos, New Mexico 87545, U.S.A.

C.D. Babcock
California Institute of Technology, Pasadena, California 91109, U.S.A.

SUMMARY

This paper describes an experimental program sponsored by the US Nuclear Regulatory Commission (NRC) that has the goal of evaluating the margin-to-failure of nuclear steel containment structures having 2:1 torispherical or ellipsoidal head geometries. An additional focus of the program is the determination of scaling laws for these heads. Pre-experimental calculations were made using the BOSOR 5 axisymmetric buckling code. Analytical parametric studies were done to determine the sensitivity of this geometry to imperfections and material properties. This information was used to develop a model of the 60 cm fabricated shells used in the testing program. An experimental apparatus is described which measured the pressure, strains and displacements during buckling of the heads. The experimental results were within 16% of the predicted value and no loss of containment was suffered by the heads themselves at pressures up to twice the bifurcation buckling pressure.

1. Introduction

Recent accident scenarios of the Three Mile Island type have caused the US Nuclear Regulatory Commission (NRC) to ask that all existing and proposed nuclear containments be assessed as to their ultimate internal pressure load carrying capacity. Evaluations have been made of the many possible failure mechanisms by the various vendors, and a number of these have been reported in the recent engineering literature. [1-2]

One type reported on is the free standing steel containment design that has a low aspect ratio head with diameter-to-height ratio (D/H) of 4:1 and with either torispherical or ellipsoidal geometry. The weakest link for loss-of-containment of this type is presumed to be failure at or near a weld in the head, initiated by knuckle buckling. Typical containment geometries for this head have diameter-to-thickness (D/t) ratios of about 1000 with knuckle radius-to-thickness (R_k/t) ratios of about 160. Calculations indicate that for this geometry, knuckle region buckling will occur at about 414 kPa (60 psi). However, there can be reserve margin above this buckling pressure if splitting does not occur.

An experimental program has been set up at the Los Alamos National Laboratory to investigate the margin-to-failure for these containment head geometries. The experiments being carried out are of three types. First, Lexan models have been constructed with this geometry to illustrate the knuckle region buckling phenomenon, since even many technical people not familiar with the deformations that the toroidal region experiences have difficulty with the concept of buckling because of internal pressure. Second, small scale experiments on 60 cm (2 ft) diameter spun steel vessels made of two torispherical heads on the ends of a cylinder are being carried out. These experiments are part of an effort to assess the scaling effects that occur for the post-buckling behavior as well as to obtain additional data on the buckling pressures for heads with containment-like geometry parameters. Third, large scale experiments on 5 m (16 ft) diameter fabricated heads will be carried out later in the year to complete the scaling effect assessment and to include the effects of field welding and construction techniques.

We will report in this paper on the preparations for, and the status of, the small scale experiments. Complete results of these experiments will be presented in this conference.

The buckling of torispherical shells under internal pressure has been studied both experimentally and analytically and this literature is reported in Refs. 3-25. However, none of this literature deals with steel shells having geometries with D/t or R_k/t ratios typical of nuclear steel containments.

2. Preliminary Analytical Modeling

A finite difference code called BOSOR 5 [8] has been used to analyze these shells. BOSOR 5 was written by David Bushnell of Lockheed, Palo Alto, and modified at Los Alamos to run on a CRAY-1 computer. It is an axisymmetric code which allows imperfection inputs, nonlinear, strain-dependent material properties, and time-varying loads and temperatures. The program can also model residual stresses due to welding and forming.

BOSOR 5 calculates the bifurcation buckling load by starting with a load value, calculating the stability determinant, incrementing the load, and recalculating the stability determinant. This process is repeated until the stability determinant changes sign. Thus the magnitude of the load steps determines the accuracy of the bifurcation load prediction. In a similar manner, the proper mode shape is determined. Once the bifurcation load is determined with an assumed mode shape, the mode shape is varied around the assumed mode shape using the previously determined load, and the minimum eigenvalue is used to decide on the proper mode shape. This algorithm is efficient for calculating buckling loads and mode shapes, but it yields no information about post-buckling behavior. The experimental portion of this program will help determine if this initial buckling load information is sufficient to predict the integrity of the shells, and the post-buckling data will be used to help predict their ultimate capacity.

Figure 1 shows the basic geometry of the computer model. The top of the cylindrical portion of the model is constrained in all six degrees of freedom. This boundary condition simulates the experimental apparatus rather than the actual reactor vessel, but analyses with only the Z direction held fixed have shown that the stress state halfway down the cylindrical region is identical to the fully restrained condition. The basic geometry is assumed to be a perfect cylinder, a perfect toroidal section, and a perfect sphere. Imperfections are incorporated into the model as perturbations to the basic geometry. Initial analysis has shown, however, that the domes are not highly sensitive to moderate imperfections. The data to which the buckling prediction from the program are very sensitive is the stress-strain relationship of the material. Consequently, actual stress-strain curves from the heads themselves are used in the calculations. This material data is critical because the buckling of mild steel torispherical heads under internal pressure occurs in the plastic regime. Thus, the buckling load is sensitive to both the yield point and the initial strain-hardening rate. With the proper stress-strain curve and an accurate description of the shell geometry, the BOSOR 5 model should accurately represent the actual shell.

3. Analytical Results

The model of Fig. 1 has an R/t ratio of approximately 500 having a radius of 30.4 cm (12 in.) and a thickness of 0.64 mm (0.025 in.). The knuckle radius is 10.4 cm (4.08 in.) and the spherical radius is 54.9 cm (21.6 in.). The height from the intersection point of the knuckle radius with the cylinder to the top of the sphere is 15.2 cm (6 in.). Thus, the shell is a 2:1 torispherical head. The cylinder height is 5.7 cm (2.25 in.). This reference surface geometry is utilized for all calculations, but alterations are superimposed upon it to account for imperfections and ridges formed by spinning. This reference geometry was used as a baseline for a number of computer runs analyzing the effects of imperfections, spinning ridges, material thickness, and material properties.

The stress-strain relationship used in the baseline case is the curve for A516 mild steel. This material has a yield stress of 276 Mpa (40,000 psi) and an ultimate tensile stress of about 496 MPa (72,000 psi) at an elongation of 25 percent. The initial plastic modulus is very small, 469 MPa (68,000 psi). The baseline computation is as close as possible to the specified dimensions of the fabricated shells but does of course differ from the actual fabricated parts.

The pressure is incremented in two steps from 0 to 276 kPa (40 psi) and then 14 kPa (2 psi) steps are taken until buckling occurs. At 276 kPa (40 psi) the shell material is still below the yield stress, and the material behavior is linear. Above the yield point the material behavior is nonlinear, and it is possible, by taking pressure increments that are too large, to step past a region where buckling is predicted. Because of the sensitivity of this phenomena to strain hardening, there may exist small regions along the stress-strain curve where buckling will occur. If a pressure increment steps beyond this point on the curve, buckling may not be predicted when in fact it would occur.

For the baseline model, buckling is predicted between 386 and 400 kPa (56 and 58 psi). This minimum buckling load occurs at 37 circumferential waves. Figure 2 shows the deformed structure with the original geometry shown as a dotted line. The deformation is exaggerated by a factor of ten. The corresponding meridional and circumferential stress resultants and the meridional moment resultant are shown in Fig. 3 as a function of arc length. From these baseline predictions, the effect of individual parameters on the buckling strength and mode shape can be determined by varying the parameters one at a time. This information can then be used to see whether the prediction for a detailed model of the fabricated shells is reasonable.

The predicted buckling load varies almost linearly with the thickness of the shell. Because buckling occurs in the plastic regime and because the tangent modulus is so low, significant deformation can occur with only small changes in stress. For the baseline case, buckling occurs when the maximum equivalent stress in only 2.07 Mpa (300 psi) greater than the yield stress. This corresponds to a plastic strain of approximately 0.005. There is only a small variation in stress across the thickness of the shell due to the meridional moments. Thus the major component of the stress is the hoop stress, which is linearly related to both the pressure and the shell thickness. For a shell thickness of 0.56 mm (0.022 in.), the predicted buckling load drops to 330 kPa to 345 kPa (48 to 50 psi).

Unlike many buckling problems, knuckle buckling due to internal pressure is insensitive to imperfections unless the amplitude of the imperfections is large with respect to their wavelength. Again, for the baseline case, the stress state in the knuckle region is the sum of the hoop stress, the meridional tensile stress, and the stresses due to the meridional moments, which are caused by the meridional tension trying to reduce the curvature of the knuckle region. Small imperfections in geometry induce additional moments upon the shell and thus alter the stress state. Depending upon their location, harmonic imperfections can either increase or decrease the maximum stress at a given point. In general they will alter the location of the point of maximum stress and thus will alter both the buckling load and the mode shape. For reasonably sized imperfections, the variations are small. For example, for a harmonic imperfection with an amplitude of 0.076 mm (.003 in.) and a wavelength of 12.7 mm (0.500 in.), the predicted buckling load is increased by 14 kPa (2 psi), while the predicted mode shape is lowered to 34 circumferential waves. For imperfections of random amplitude and wavelength, the same concepts apply since the random imperfections can be considered as the superposition of a set of harmonic imperfections.

While knuckle buckling in general is quite sensitive to the strain-hardening properties of the shell material, this particular geometry is less sensitive to stress-strain properties than some others. The ratio of knuckle radius to sphere radius is small enough that buckling occurs for both elastic-purely plastic materials and completely elastic materials although the predicted buckling pressure is twice as high for the elastic case as for the elastic-plastic case with a yield stress of 276 MPa (40,000 psi). The buckling pressure varies approximately linearly with yield stress for this geometry. For shells with larger knuckle radius-to-sphere radius ratios this relationship does not hold. Bushnell in Ref. 9 shows diagrams of the variation of meridional and circumferential stress resultants as functions of tangent modulus, thickness-to-radius ratio, and knuckle radius-to-height ratio. He demonstrates that for certain geometries, relatively small changes in material properties can completely change the character of the shell's response to internal pressurization. However, this is not the case for the 2:1 torispherical geometry. The material properties for the A516 mild steel also tend to reduce the sensitivity. The tangent modulus is extremely low for this material such that even if it were doubled for a particular sample, the effect on the buckling pressure would be small. Thus for this geometry and material, the yield stress is the most significant material parameter affecting the buckling load and the buckling pressure varies almost linearly with yield stress.

The effect of circumferential ridges on buckling strength was also investigated since such ridges are normally encountered in spun materials. Only relatively small ridges were considered since the ridges would not be found on large structures and small spun heads should have rather limited spinning marks. Again, since the circumferential stresses are dominated by the hoop stresses and the existence of ridges does not alter the cross sectional area, the effect of the ridges is not significant. In addition since buckling occurs in the plastic regime, the stress across the thickness is approximately constant as bending occurs when a buckle forms, and thus the resistance to buckling increases linearly with distance from the neutral plane rather than to the third power as would be the case of elastic buckling. For ridges of amplitude 0.152 mm (0.006 in.) and wavelength of 1.27 mm (0.050 in.) the buckling pressure is increased less than 14 kPa (2 psi).

With the described parametric studies as background, a model of a fabricated shell can be created including the effects of imperfections, deviations from baseline geometry, material properties, shell thickness, and spinning ridges with some confidence in the results. The first test shell was modeled. The shell's sphere radius was slightly smaller than specified making the height to diameter ratio slightly larger. The most significant imperfections were about 0.51 mm (0.020 in.) in amplitude with a wavelength of several centimeters. The material thickness varies from 0.56 mm (0.022 in.) to 0.61 mm (0.024 in.) averaging 0.58 mm (0.023 in.). This shell was only stress-relieved rather than annealed after forming so that the stress-strain curve is altered due to strain hardening. The plastic strain during spinning was approximated by comparing the circumference at the center of the knuckle with the circumference of a circle with a radius equivalent to the arc length from the top of the shell to the center of the knuckle. The stress-strain curve was then shifted to the left by the equivalent plastic strain. This gave a yield stress of 299 MPa (43,300 psi) and a tangent modulus of approximately 965 MPa (140,000 psi). The decreased thickness should lower the buckling pressure approximately 34-41 kPa (5-6 psi) while the increased yield strength should increase the pressure by 20 to 27 kPa (3 to 4 psi). The other effects should be small. The predicted value from the BOSOR 5 program is 372 to 386 kPa (54 to 56 psi).

4. Experimental Techniques

Several shells with a 2:1 torispherical head geometry and a diameter to thickness ratio of approximately 1000 have been fabricated by spinning over a machined wooden mandrel. Two heads are epoxied into opposite sides of a machined aluminum ring to form a pressure vessel. The heads were epoxied because welds could not be made to scale on such small vessels. The heads are filled with water and pressurized with nitrogen. Pressure data, displacement data, and strain gage data are all recorded automatically with a Hewlett Packard 9825 computer. Figure 4 shows the experimental apparatus.

Because the shells are fabricated from mild steel by spinning over a mandrel, they are significantly work-hardened and must be heat treated. One pair of shells was stress-relieved in air for one hour at 650^{o}C (1200^{o}F). The remaining five shells were annealed at 900^{o}C (1650^{o}F) for two hours in an argon atmosphere. One of the annealed shells is being cut up for material property samples. A bleed valve was installed in one of the heads in each set. After installation of the internal strain gages, the heads were epoxied into a 12.7 mm (0.5 in.) deep groove in opposite sides of a machined aluminum mounting ring using a Devcon F-3 super liquid aluminum epoxy. The shear strength of the epoxy is sufficient to make the bond to the aluminum ring stronger than the metal itself. The shells formed in this manner show spinning marks with a depth of about 0.1 mm (0.004 in.) and a spacing of 2.5 mm (0.100 in.).

The shells are filled with water and pressurized with nitrogen flowing through a needle valve. The amount of nitrogen downstream of the valve is kept to a minimum to limit the energy storage in the pressurized shell. Fluid enters the vessel through the aluminum mounting ring so that the effect of hoses and couplings on the shell is eliminated. The pressure is controlled by a regulator on a regular high pressure nitrogen bottle. The pressure at the shell is monitored with a calibrated Validyne pressure transducer. The pressure data is visually displayed and also recorded by the HP 9825 computer.

Strain gages are mounted on both the inside and the outside surface of the shell. Since the vessel is pressurized with tap water, the interior gages are insulated with Gagekote. All wires are brought out through the mounting ring with Conax pressure fittings. All strain gages are calibrated prior to a test run, with the calibration data being read directly by the computer. This calibration data is used to reduce the strain gage output voltage to strains, on line, as the data is taken.

Displacement measurements are made at 8 circumferences on each head. Eight Vernitech linear potentiometers are mounted on a moveable arm. The potentiometers are spring-loaded against the head. The arm is solidly attached to a shaft which is mounted on two tapered roller bearings. The shaft is driven by a Superior Electric SloSyn stepping motor through a worm gear. The preload on the bearings is adjustable to eliminate shaft wobble, and the worm to gear centerline distances are adjustable to eliminate backlash. Shaft wobble can be completely eliminated, and backlash can be held to less than 0.1 degrees. The potentiometers have been calibrated and the maximum error for any potentiometer using a linear curve fit for this data is $\pm$ 0.025 mm ($\pm$ 0.001 in.). The maximum error using a fourth order curve fit is $\pm$ 0.01 mm ($\pm$ 0.0004 in.). The curve fit for each potentiometer is fed into the computer and is used to translate the voltage into a deflection during the test. The stepping motors are controlled by the computer. They are moved to a prescribed position and stopped before a reading is taken. After the pressure is incremented, the arm is swept around the shell, and a potentiometer reading is taken every 3^{o} around the circumference.

All of the data (pressure, displacement, and strain) is taken by the HP 9825 computer using an HP-3052A data acquisition system. This data acquisition system consists of a 50 channel scanner, a high-resolution digital voltmeter, and a floppy disk drive for data storage. Both the scanner and digital voltmeter are triggered from the computer. A

4-into-1 relay network is used to multiplex the 96 channels of strain gage data. This relay multiplexer is also controlled by the computer. Calibration data for both the strain gages and the potentiometers is contained within the computer program to allow on-line data conversion and printout. The data is stored as strain, displacement, and pressure. The shells are initially measured on a precision X,Y,Z digitizer table and this information is used to zero the potentiometers so that the displacement data is referenced to the actual shell rather than the prescribed geometry.

5. Experimental Results

The only shells that have been tested to date are the set of stress-relieved shells described in the analytical results section, and the analysis of these results is not yet complete. However, the buckling pressure for the bottom head was 317 kPa (46 psi) while the top head buckled at 441 kPa (64 psi). These pressures were the points at which buckles were first discernable from the computer plots. Slightly higher values were necessary to obtain readily visible buckles. The number of buckles was small, approximately 12 to 15, but their wavelength was fairly consistent with the predicted mode shape. Figure 5 shows a picture of the buckled head. Clearly there are large areas of unbuckled material between rather short wavelength buckles. The buckles protrude outward in all cases which is exactly opposite to our experience with Lexan shells which buckle elastically. The actual buckling pressures differed from the predicted values by ± 16%. This difference is most likely due to variations of the material thickness in the knuckle region. No thickness measurements were taken in the knuckle region because we had no convenient method for taking them. Measurements will be made on the subsequent tests using an ultrasonic thickness gauge which is currently on order.

A major emphasis in this program is an experimental determination of the margin-to-failure over and above the bifurcation buckling pressure. The vessel was pressurized past the initial buckling point. At approximately 344 kPa (50 psi) a small leak developed where the shell was bonded to the support ring. The leak was in the epoxy used to bond the head onto the support ring. Pressurization was continued until the buckles were too high to measure with the linear potentiometers. The pressure was released and the potentiometer arms were removed. The vessel was again pressurized to determine the containment failure point. The buckles deepened but never became sharp. At approximately 689 kPa (100 psi) a large crack developed in the epoxy bonding the lower head to the support ring and the test was discontinued. No failure had occurred in the heads themselves.

It is clear that the margin-to-failure over buckling for the ductile heads without welds may be quite large and that a different bonding system must be developed to test these heads to failure. The prediction of buckling pressure was reasonably good, but with additional information about material properties and material thickness variations in the knuckle region, our predictive capability for this kind of buckling should improve.

References

[1] Sundararjan, C., ed., "Safety and Reliability of Pressure Components," 1982 Pressure Vessel and Piping Conference Bound Volume, PVP-62, BK. No. 400219.

[2] Bernstein, M. D., Iotti, R. C., VonRiesemann, ed., Advances in Containment Design and Analysis, ASME/ANS Joint Conference Proceedings, Portland, OR, July 26-28, 1982.

[3] Bushnell, D., "Buckling of Shells - Pitfall for Designers," AIAA Journal, Sept. 1981.

[4] Mescall, J., "Stability of Thin Torispherical Shells Under Uniform Internal Pressure," NASA TN D-1510, Collected Papers on Instability of Shell Structures, pp 671-692 (Dec. 1962).

[5] Adachi, J., and Benicek, M., "Buckling of Torispherical Shells Under Internal Pressure," Experimental Mechanics, Vol. 4, No. 8, pp 217-222 (Aug. 1964).

[6] Thurston, G., and Holston, A. A., Jr., "Buckling of Cylindrical Shell End Closures by Internal Pressure," NASA CR-540 (July 1966).

[7] Brown, K. W., and Kraus, H., "Stability of Internally Pressurized Vessels with Ellipsoidal Heads," presented at 2nd National Congress on Pressure Vessels and Piping Technology, San Francisco (June 23-27, 1975).

[8] Bushnell, D., and Galletly, G. D., "Comparisons of Test and Theory for Nonsymmetric Elastic-Plastic Buckling of Shells of Revolution," Int. J. Solids Struct., Vol. 10, pp 1271-1285 (1974).

[9] Bushnell, D., and Galletly, G. D., "Stress and Buckling of Internally Pressurized Torispherical Vessel Heads--Comparisons of Test and Theory," ASME J. Pressure Vessel Technology, Vol. 99, pp 39-53 (Feb. 1977).

[10] Lagae, G., and Bushnell, D., "Elastic-Plastic Buckling of Internally Pressurized Torispherical Vessel Heads," Nuclear Engineering and Design, Vol. 48, pp 405-414 (1978).

[11] Galletly, G. D., "Internal Pressure Buckling of Very Thin Torispherical Shells--A Comparison of Experiment and Theory," 3rd SMIRT Conf., London, Paper G2/3 (1975).

[12] Galletly, G. D., "Elastic and Elastic-Plastic Buckling of Internally-Pressurized 2:1 Ellipsoidal Shells," ASME Paper 78-PVP-47 (June 1978).

[13] Kirk, A., and Gill, S. S., "The Failure of Torispherical Ends of Pressure Vessels Due to Instability and Plastic Deformation--An Experimental Investigation," Int. J. Mech. Sci., Vol. 17, pp 525-544 (1975).

[14] Patel, P. R. and Gill, S. S., "Experiments on the Buckling Under Internal Pressure of Thin Torispherical Ends of Cylindrical Pressure Vessels," Int. J. Mech Sci., Vol. 20, pp 159-175 (1978).

[15] Esztergar, E., "Development of Design Rules for Dished Pressure Vessel Heads," Welding Research Council Bulletin, 215 (April 1976).

[16] Ranjan, G. V., and Steele, C. R., "Analysis of Knuckle Region Between Two Smooth Shells," JAM, Vol 42, pp 853-857.

[17] Ranjan, G. V., and Steele, C. R., "Analysis of Torispherical Pressure Vessels," ASCE, Eng. Mech. Div., Vol. 102, No. EM4, Aug. 1976, pp 643-657.

[18] Steel, C. R., and Skogh, J., "Slope Discontinuities in Pressure Vessels," Journal of Applied Mechanics, Vol. 37, Trans. ASME, Vol. 92, Series E, pp 587-595, Sept. 1970.

[19] Calladine, C. R., "Creep in Torispherical Pressure Vessel Heads," Creep in Structures, IUTAM-Symposium, Gothenburg, 1970, pp 247-268.

[20] Adachi, J., and Benicek, M., "Buckling Instability of Pressurized Torispherical Shells," Proceedings of the Army Symposium on Solid Mechanics, Sept. 1968, pp 159-171.

[21] Benicek, M., and Adachi, J., "Measured Nonlinear Distributions in Pressurized Torispherical Shells," Proceedings of the Army Symposium on Solid Mechanics, Sept. 1968, pp 173-188.

[22] Clark, R. A., "On the Theory of Thin Elastic Toroidal Shells, "Journal of Mathematics and Physics," Vol. 29, 1950, pp 146-178.

[23] Steele, C. R., "Geometric Optics Approach to Shell Analysis," Proceedings of the Annual Meeting, Society of Engineering Science, Raleigh, NC, Nov. 1973.

[24] Stoddart, J. S., and Owen, B. S., "Stresses in a Torispherical Pressure Vessel Head," Meeting on Stress Analysis Today, Stress Analysis Group, Institute of Physics, 1965.

[25] Mescall, J., "On a Particular Integral for Toroidal Shells Under Uniform Pressure," Journal of Applied Mechanics, Vol. 30, No. 1, March 1963.

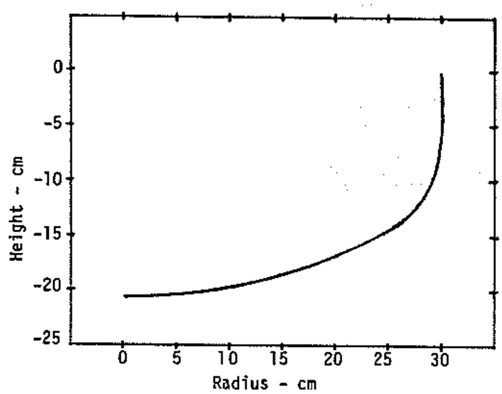

Fig. 1. Initial undeformed structure.

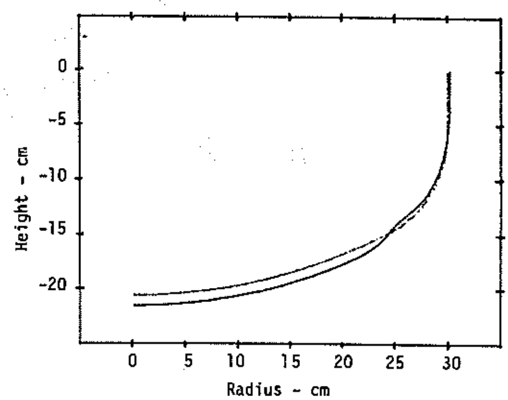

Fig. 2. Deformed geometry - 400 kPa.

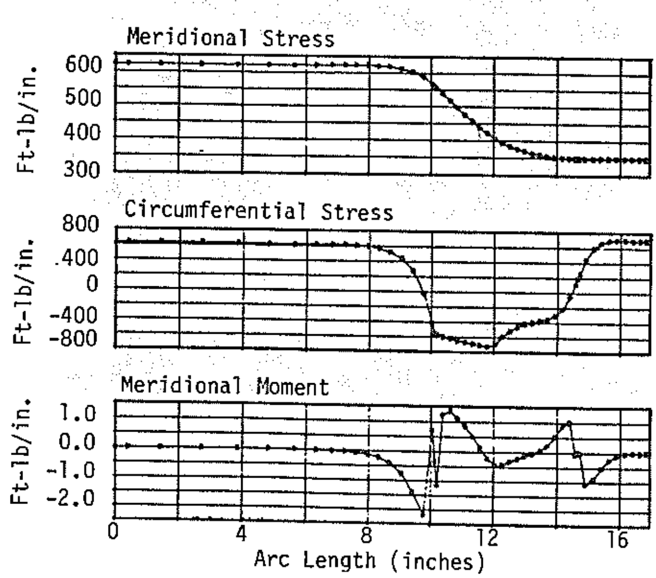

Fig. 3. Stress and moment resultants.

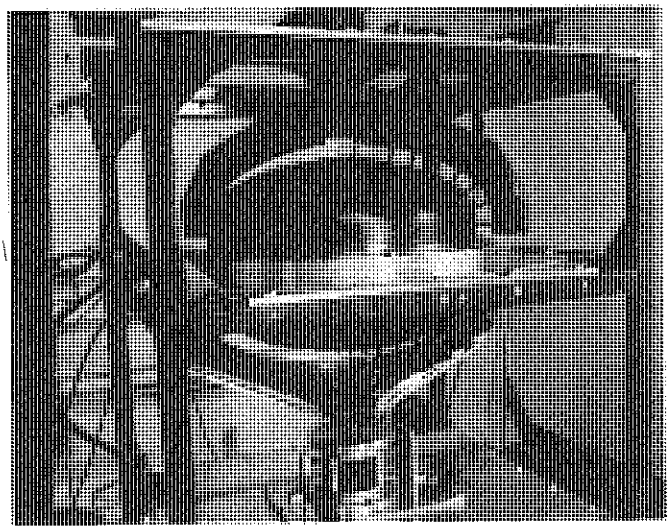

Fig. 4. Pressurization and measurement apparatus.

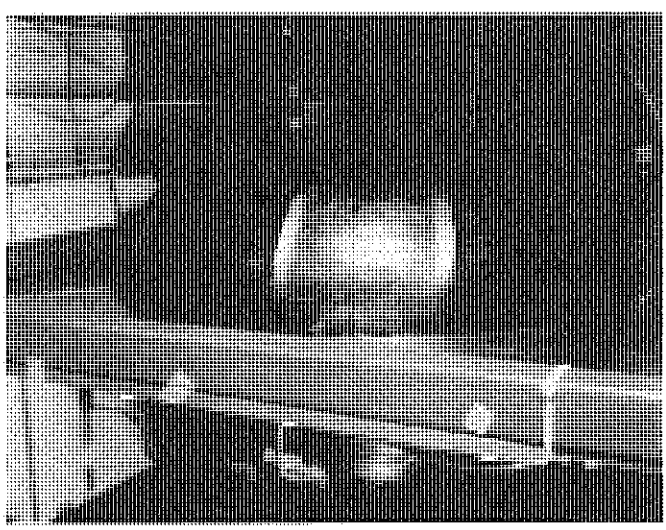

Fig. 5. Buckles formed in lower head.